VIBRATIONS OF LATTICE STRUCTURES AND PHONONIC BAND GAPS

by P. G. MARTINSSON

(*Texas Institute for Computational and Applied Mathematics, University of Texas at Austin, Austin,* TX 78712*, USA*)

and A. B. MOVCHAN

(*Department of Mathematical Sciences, University of Liverpool, Liverpool* L69 3BX)

Summary

Elastic waves in lattice structures are considered. The propagating modes as well as filtering properties of lattices are analysed. Special attention is paid to the connection between microstructural geometry and the presence of so-called 'phononic band gaps', intervals of frequencies for which no propagating wave modes exist.

1. Introduction

In this paper we will demonstrate that for many mechanical lattice structures there are intervals of frequencies for which no propagating elastic waves exist. This raises the possibility of designing materials, or structures, that can completely block mechanical waves of certain frequencies. We will present a method of analysis that can be used to determine such band gaps and then show how lattices can be constructed that have band gaps around prescribed frequencies.

There are many observations of band-gap phenomena in nature; in the classical literature (see, for example, (**1**, **2**)) it has been shown that real life molecular structures may exhibit band gaps on the dispersion diagrams corresponding to both acoustic and electromagnetic waves (referred to as phononic and photonic band gaps, respectively). A comprehensive bibliography including more than one thousand articles on photonic band structures has been compiled (**3**). Theoretical and numerical studies based on the plane wave expansion method were published by Sigalas and co-workers (**4** to **6**), who considered scalar problems for acoustic wave band structures as well as vector problems for elastic waves in plates containing periodic sets of inclusions. For continuum elastic structures the phononic band-gap phenomena were studied in (**7**), where a generalization of the Rayleigh method was developed to analyse the elastic wave propagation through a two-dimensional array of circular voids.

It is evident that one can establish a correspondence between continuum structures and discrete lattices. For example, for the case of a normal incidence of an anti-plane wave on a stack of two types of elastic layers (Fig. 1a) we can assume that the layers of one of the groups are thin and soft. In this case, it can be shown (**8**) that asymptotically the dispersion equation for this structure would be equivalent to the one corresponding to a bi-atomic one-dimensional chain of particles of different mass connected by weightless elastic springs (Fig. 1b). The dispersion diagram given in Fig. 2
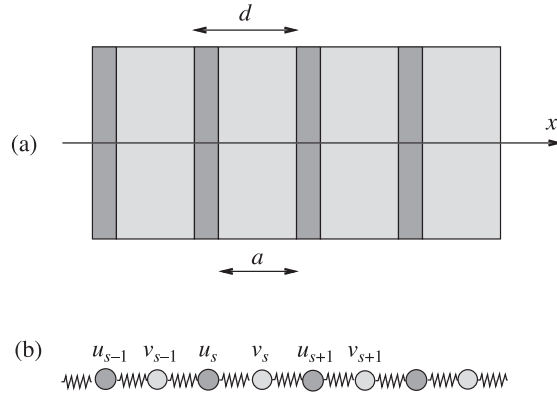
Fig. 1 (a) One-dimensional array, of period d, involving two types of layers, of thickness a and $(d-a)$, and (b) a two-particle system with springs

shows the normalized frequency versus the magnitude of the Bloch vector and exhibits the band gap between the acoustic and optical modes for this one-dimensional problem. The comparison of certain anti-plane problems for continuous systems in two dimensions and two-dimensional lattice structures was also included in (**8**). It is noted that the analysis of lattice structures is easy compared to numerical computations for continuum systems of complicated geometries; on the other hand the lattice structure may exhibit the physical phenomena similar to continuum structures, and hence it is important to be able to evaluate the transmission and reflection characteristics of lattice structures.

We emphasize the analysis of vector problems of elasticity for lattice structures and pay particular attention to the effects of phononic band gaps. Our analysis is restricted to two dimensions but the methodology easily generalizes to three-dimensional structures. The plan of the paper is as follows. We begin by considering elementary examples of membrane-like lattices with different assumptions related to the mass distribution along the strings. In section 2 we analyse in-plane elastic vibrations of degenerate and non-degenerate bi-atomic lattice structures that exibit phononic band gaps. A general approach to spectral problems for lattice structures is presented in section 3. This approach is used in section 4 to design structures which possess band-gap frequencies of given magnitude. It is specifically noted that the band-gap phenomena are associated with the presence of standing waves within the structure.

1.1 *A membrane-like lattice*

We consider illustrative examples for a lattice with the square geometry illustrated in Fig. 3. We think of the lines of the lattice as strings with an axial force F, and a weight-per-length density ρ. The strings are attached to each other at the nodal points. We consider harmonic vibrations of this lattice with displacements of the strings and the nodes in the direction perpendicular to the plane of the lattice. Our goal is to determine the eigenmodes and to look for band gaps in the spectrum.

Homogeneous strings of constant density.   Since the domain is infinite and the vibrations are quasi-periodic in space we can restrict our attention to a unit cell, as illustrated in Fig. 3. Let $u^{(j)}$,
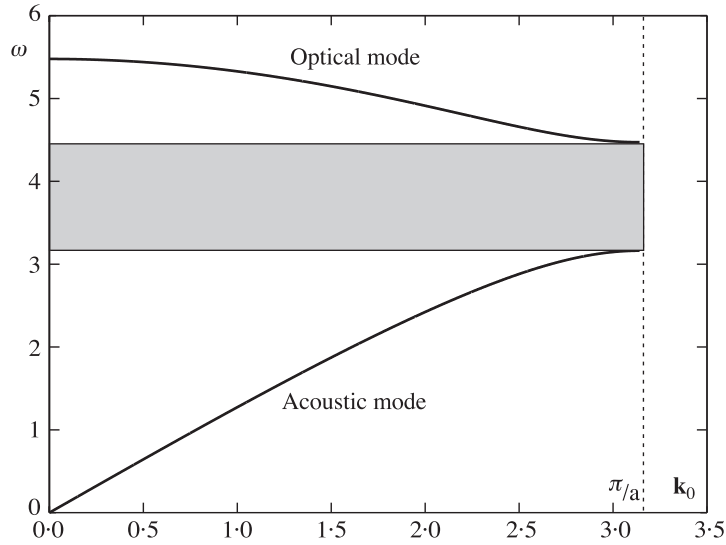
Fig. 2 Acoustic and optical branches for a one-dimensional array of particles of mass $m_1 = 1$ and $m_2 = 2$ connected by springs of length $a = 1$ and stiffness $c = 10$. The magnitude of the Bloch vector is along the horizontal axis and the radian frequency is along the vertical axis
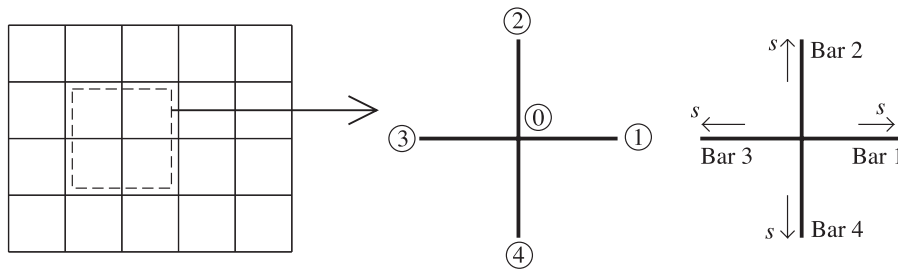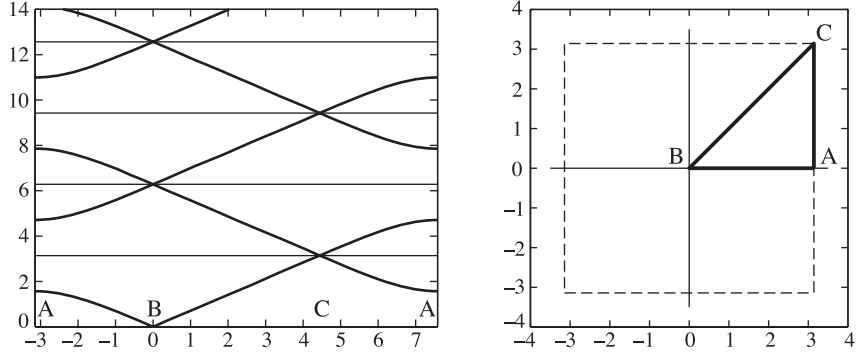

Fig. 3 Square lattice with mass distributed along the bars

$j = 0, 1, \ldots, 4$, denote the displacement of the nodes, where j is the index shown in the figure. Let $w^{(j)}(x, t)$ denote the displacement of the string connecting node 0 to node j, with $x \in (0, l)$ measured as shown in the figure and t denoting time. Then Newton's second law reads

$$F\frac{d^2 w^{(j)}}{dx^2} = \rho \frac{d^2 w^{(j)}}{dt^2}.$$

As we consider time-harmonic oscillations, say of radian frequency ω, we have $d^2 w^{(j)}/dt^2 = -\omega^2 w^{(j)}$ and obtain

$$\frac{d^2 w^{(j)}}{dx^2} + \frac{\omega^2}{v^2} w^{(j)} = 0,$$

Fig. 4 Dispersion diagram for the square lattice with distributed mass. The non-dimensionalized solutions $\omega l/v$ are plotted against $\mathbf{k}$ along the contour shown to the right

where $v = \sqrt{F/\rho}$ is the internal group-velocity of the strings. The boundary conditions are $w^{(j)}(0) = u^{(0)}$ and $w^{(j)}(l) = u^{(j)}$. Considering first the case $\sin(\omega l/v) \neq 0$ we find that

$$w^{(j)}(x) = u^{(0)}\cos Kx + \left(u^{(j)} - u^{(0)}\cos Kl\right)(\sin Kx)/(\sin Kl) \quad \text{with} \quad K = \omega/v.$$

Equilibrium of the central node now reads

$$0 = \sum_{n=1}^{4} \frac{dw^{(j)}}{dx}\bigg|_{x=0} = \left(u^{(1)} + u^{(2)} + u^{(3)} + u^{(4)} - 4u^{(0)}\cos Kl\right)/(\sin Kl). \tag{1}$$

Looking for waves with a Bloch vector $\mathbf{k} = (k_1, k_2)$ we have the quasi-periodicity conditions

$$u^{(1)} = e^{-ik_1 l}u^{(0)}, \quad u^{(2)} = e^{-ik_2 l}u^{(0)}, \quad u^{(3)} = e^{ik_1 l}u^{(0)} \quad \text{and} \quad u^{(4)} = e^{ik_2 l}u^{(0)}.$$

Substituting these in (1) we obtain the equation

$$\cos k_1 l + \cos k_2 l - 2\cos Kl = 0.$$

For the case $\sin Kl = 0$ there exist, for any $\mathbf{k}$, standing wave modes corresponding to internal vibrations of the strings, with no associated nodal displacements. The total dispersion equation therefore takes the form

$$\sin(Kl)(\cos k_1 l + \cos k_2 l - 2\cos Kl) = 0.$$

Note that in the limit $\mathbf{k} \to 0$ the dispersion equation has the asymptotic solution $|\mathbf{k}| = \sqrt{2}\,\omega/v$, the same dispersion equation as for a continuous membrane with group velocity $v/\sqrt{2}$.

Given $\mathbf{k} \in (-\pi, \pi)^2$ the dispersion equation allows us to determine all frequencies ω such that there is a vibration mode with frequency ω and the Bloch vector $\mathbf{k}$. In Fig. 4 we plot the solutions ω versus the $\mathbf{k}$s along the path shown to the right in the figure. It is clear that no complete band gaps exist.
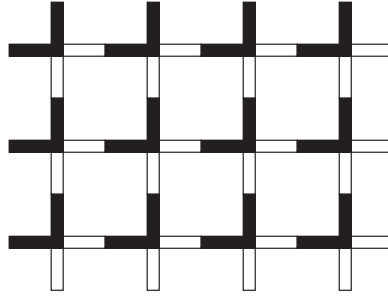
Fig. 5 Lattice consisting of strings with non-constant density. The white parts of the strings have density ρ, the black have density ρ/α^2
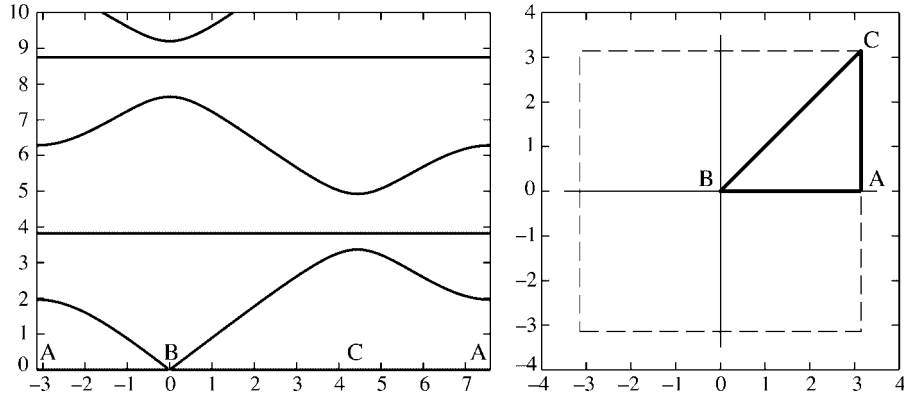
Fig. 6 Dispersion diagram similar to the one shown in Fig. 4 but for the lattice with strings of varying density, $\alpha = 2$

Inhomogeneous strings. We next consider a structure similar to the one analysed above but where the strings are not homogeneous; the density has been changed from ρ to ρ/α^2 in half the bar, as illustrated in Fig. 5. In this case we derive (see Appendix A) the dispersion equation

$$\left[\cos \frac{Kl}{2} \sin \frac{Kl}{2\alpha} + \frac{1}{\alpha} \cos \frac{Kl}{2\alpha} \sin \frac{Kl}{2}\right]$$
$$\times \left[\frac{1}{\alpha}\left(\cos k_1 l + \cos k_2 l - 2\cos \frac{Kl}{2} \cos \frac{Kl}{2\alpha}\right) + \left(1 + \frac{1}{\alpha^2}\right) \sin \frac{Kl}{2} \sin \frac{Kl}{2\alpha}\right] = 0, \quad (2)$$

with $K = \omega/v$. One very interesting feature here is that the first factor captures exactly the eigenfrequencies of the inhomogeneous string with fixed ends. As shown in Fig. 6, around these frequencies there are typically complete band gaps. This means that no waves with frequencies close to the eigenfrequencies of the composite bars can propagate through the structure.

The two elementary examples considered above provide sufficient motivation for analysis of trapped modes and phononic band gaps in elastic structures. These vector problems are considered below.

2. Mechanical lattices of two kinds

Every periodic lattice is characterized by an irreducible cell and a corresponding stiffness matrix A associated with this cell. Thinking of the members of the lattice as beams we know that the matrix A splits into two components, $A = A_{\text{axial}} + A_{\text{bending}}$, with the first representing the axial stiffness of the beams and the second representing the bending stiffness. If the bars are slender we know that the axial stiffness is much higher than the bending stiffness. If A_{axial} has full rank when restricted to the translational degrees of freedom it will entirely dominate the problem and in this case we usually neglect the effect of A_{bending} and solve only for the translational degrees of freedom. We refer to these structures as *truss structures*. On the other hand, if A_{axial} does not have full rank (when restricted to the translational degree of freedom) we do need to keep A_{bending} in order to maintain structural integrity. Note that in this case A will be badly conditioned and we will expect the lattice to exhibit strongly anisotropic behaviour. Such structures we refer to as *frame structures*. In the next two subsections we will study one each of these two kinds of structures. We will try to make plausible the claim that even though band gaps do exist in some truss structures they are more typical for the frames of the type considered in section 2.2.

2.1 A bi-atomic triangular lattice

Consider the triangular lattice illustrated in Fig. 7. It consists of bars with an axial stiffness c connected with pin-joints. At the nodes with small dots there is a mass m_1 and at the big dots there is a mass m_2. The lattice has an irreducible unit cell Ω whose integer translations along the lattice vectors $\mathbf{t}^{(1)} = (2l, 0)$ and $\mathbf{t}^{(2)} = (l/2, \sqrt{3}l/2)$ cover the whole plane

$$\mathbb{R}^2 = \bigcup_{n \in \mathbb{Z}^2} (\Omega + n_1 \mathbf{t}^{(1)} + n_2 \mathbf{t}^{(2)}).$$

We identify the coordinates of the two nodes in Ω as $\mathbf{x}^1 = (0, 0)$ and $\mathbf{x}^2 = (l, 0)$; then the node $\kappa \in \{1, 2\}$ in cell $\mathbf{n} \in \mathbb{Z}^2$ has coordinates $\mathbf{x}^{(\mathbf{n}, \kappa)} = \mathbf{x}^\kappa + T\mathbf{n}$ where $T = [\mathbf{t}^{(1)}, \mathbf{t}^{(2)}]$.

We let $\mathbf{u}^{(\mathbf{n}, \kappa)} = (u_1^{(\mathbf{n}, \kappa)}, u_2^{(\mathbf{n}, \kappa)})^\mathrm{T}$ denote the displacement of node $(\mathbf{n}, \kappa)$. Introducing the unit vectors

$$\mathbf{a}_j = \left(\cos \tfrac{2}{3}(j-1)\pi, \; \sin \tfrac{2}{3}(j-1)\pi\right)^\mathrm{T}, \quad j = 1, 2, 3, \tag{3}$$

and setting $\mathbf{e}_1 = (1, 0)^\mathrm{T}$, $\mathbf{e}_2 = (0, 1)^\mathrm{T}$ we can express the equations of motion for the case of harmonic oscillations (of radian frequency ω) as

$$\begin{aligned}
\omega^2 m_1 \mathbf{u}^{(\mathbf{n}, 1)} &= c\, \mathbf{a}_1 \mathbf{a}_1^\mathrm{T} (2\mathbf{u}^{(\mathbf{n}, 1)} - \mathbf{u}^{(\mathbf{n}, 2)} - \mathbf{u}^{(\mathbf{n} - \mathbf{e}_1, 2)}) \\
&\quad + c\, \mathbf{a}_2 \mathbf{a}_2^\mathrm{T} (2\mathbf{u}^{(\mathbf{n}, 1)} - \mathbf{u}^{(\mathbf{n} + \mathbf{e}_2, 1)} - \mathbf{u}^{(\mathbf{n} - \mathbf{e}_2, 1)}) \\
&\quad + c\, \mathbf{a}_3 \mathbf{a}_3^\mathrm{T} (2\mathbf{u}^{(\mathbf{n}, 1)} - \mathbf{u}^{(\mathbf{n} - \mathbf{e}_1 + \mathbf{e}_2, 2)} - \mathbf{u}^{(\mathbf{n} - \mathbf{e}_2, 2)}), \\
\omega^2 m_2 \mathbf{u}^{(\mathbf{n}, 2)} &= c\, \mathbf{a}_1 \mathbf{a}_1^\mathrm{T} (2\mathbf{u}^{(\mathbf{n}, 2)} - \mathbf{u}^{(\mathbf{n} + \mathbf{e}_1, 1)} - \mathbf{u}^{(\mathbf{n}, 1)}) \\
&\quad + c\, \mathbf{a}_2 \mathbf{a}_2^\mathrm{T} (2\mathbf{u}^{(\mathbf{n}, 2)} - \mathbf{u}^{(\mathbf{n} + \mathbf{e}_2, 2)} - \mathbf{u}^{(\mathbf{n} - \mathbf{e}_2, 2)}) \\
&\quad + c\, \mathbf{a}_3 \mathbf{a}_3^\mathrm{T} (2\mathbf{u}^{(\mathbf{n}, 2)} - \mathbf{u}^{(\mathbf{n} + \mathbf{e}_2, 1)} - \mathbf{u}^{(\mathbf{n} + \mathbf{e}_1 - \mathbf{e}_2, 1)}).
\end{aligned}$$
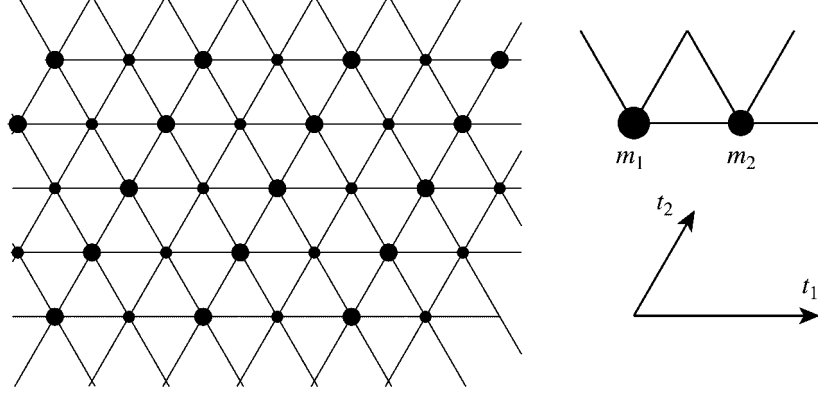
Fig. 7 Triangular bi-atomic lattice. To the right we illustrate the irreducible unit cell and the lattice vectors

Applying the condition of quasi-periodicity, $\mathbf{u}^{(\mathbf{n}+\mathbf{m},\kappa)} = e^{i\mathbf{k}\cdot T\mathbf{m}}\mathbf{u}^{(\mathbf{n},\kappa)}$, we obtain

$$\omega^2 m_1 \mathbf{u}^{(\mathbf{n},1)} = c\left[2\mathbf{a}_1\mathbf{a}_1^{\mathrm{T}} + 4\sin^2\phi\,\mathbf{a}_2\mathbf{a}_2^{\mathrm{T}} + 2\mathbf{a}_3\mathbf{a}_3^{\mathrm{T}}\right]\mathbf{u}^{(\mathbf{n},1)}$$
$$+ c\left[(1+e^{-2ik_1 l})\mathbf{a}_1\mathbf{a}_1^{\mathrm{T}} + (e^{-i\psi_1}+e^{-i\psi_2})\mathbf{a}_3\mathbf{a}_3^{\mathrm{T}}\right]\mathbf{u}^{(\mathbf{n},2)},$$
$$\omega^2 m_2 \mathbf{u}^{(\mathbf{n},2)} = c\left[2\mathbf{a}_1\mathbf{a}_1^{\mathrm{T}} + 4\sin^2\phi\,\mathbf{a}_2\mathbf{a}_2^{\mathrm{T}} + 2\mathbf{a}_3\mathbf{a}_3^{\mathrm{T}}\right]\mathbf{u}^{(\mathbf{n},1)}$$
$$+ c\left[(1+e^{2ik_1 l})\mathbf{a}_1\mathbf{a}_1^{\mathrm{T}} + (e^{i\psi_1}+e^{i\psi_2})\mathbf{a}_3\mathbf{a}_3^{\mathrm{T}}\right]\mathbf{u}^{(\mathbf{n},2)},$$

where

$$\phi = \tfrac{1}{4}(k_1 l + \sqrt{3}k_2 l), \quad \psi_1 = \tfrac{1}{2}(3k_1 l - \sqrt{3}k_2 l) \quad \text{and} \quad \psi_2 = \tfrac{1}{2}(k_2 l + \sqrt{3}k_2 l).$$

Introducing the vector $\mathbf{u}^{(\mathbf{n})} = [\mathbf{u}^{(\mathbf{n},1)}, \mathbf{u}^{(\mathbf{n},2)}]^{\mathrm{T}} \in \mathbb{R}^4$, we write this compactly as

$$\omega^2 M\mathbf{u}^{(\mathbf{n})} = \sigma(\mathbf{k})\mathbf{u}^{(\mathbf{n})}, \tag{4}$$

where we defined a mass matrix $M = \mathrm{diag}\{m_1, m_1, m_2, m_2\}$ and a 4×4 stiffness matrix $\sigma(\mathbf{k})$. The entries of $\sigma(\mathbf{k})$ are given by

$$\sigma_{11}(\mathbf{k}) = c\begin{bmatrix} \frac{5}{2} + \sin^2\phi & -\frac{1}{2}\sqrt{3} + \sqrt{3}\sin^2\phi \\ -\frac{1}{2}\sqrt{3} + \sqrt{3}\sin^2\phi & \frac{3}{2} + 3\sin^2\phi \end{bmatrix},$$

$$\sigma_{12}(\mathbf{k}) = c\begin{bmatrix} 1 + e^{2ik_1 l} + \frac{1}{4}e^{-i\psi_1} + \frac{1}{4}e^{-i\psi_2} & \frac{1}{4}\sqrt{3}e^{-i\psi_1} + \frac{1}{4}\sqrt{3}e^{-i\psi_2} \\ \frac{1}{4}\sqrt{3}e^{-i\psi_1} + \frac{1}{4}\sqrt{3}e^{-i\psi_2} & \frac{3}{4}e^{-i\psi_1} + \frac{3}{4}e^{-i\psi_2} \end{bmatrix},$$
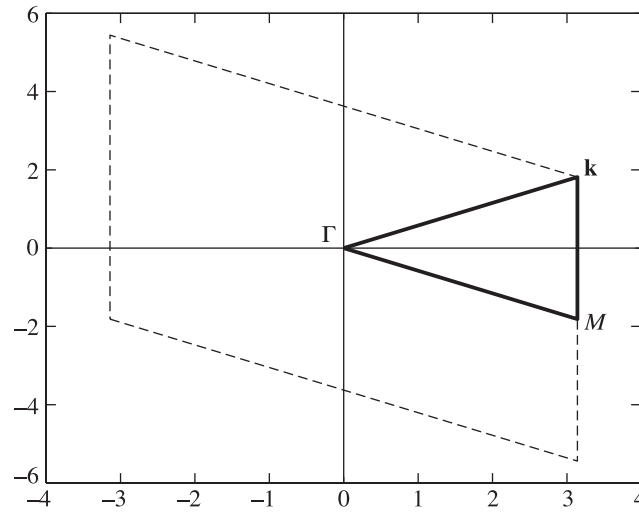
using that $\sigma_{22}(\mathbf{k}) = \sigma_{11}(\mathbf{k})$ and $\sigma_{21}(\mathbf{k}) = \sigma_{12}(\mathbf{k})^\star$. Equation (4) has non-trivial solutions if and only if

$$\det\left\{\sigma(\mathbf{k}) - \omega^2 M\right\} = 0. \tag{5}$$

This equation is referred to as the dispersion equation of the lattice.
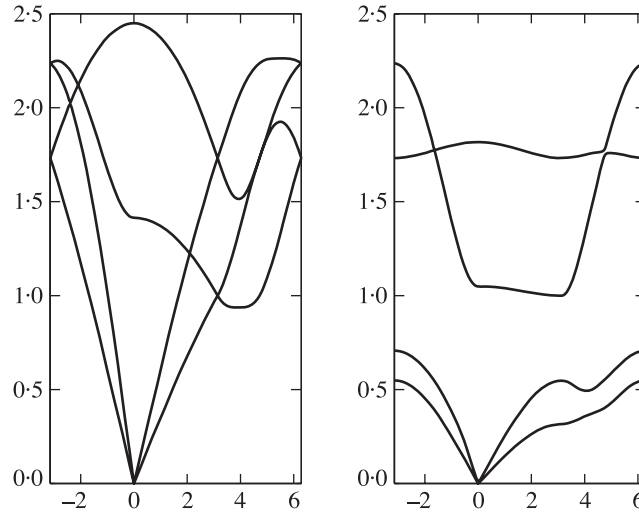
Fig. 8 Eigenfrequencies for the triangular biatomic lattice with $c = 1$. In the left graph, $m_1 = m_2 = 1$, in the right, $m_1 = 1, m_2 = 10$

Fig. 9 The reciprocal lattice is contained in the dashed parallelogram. The thick line illustrates the contour along which the eigen-frequencies are plotted

Equation (5) has been solved numerically for some different combinations of masses (the spring constant c was set to unity). As illustrated in the left graph of Fig. 8 there is no band gap when $m_1 = m_2 = 1$. In this graph **k** follows the path illustrated in Fig. 9. By increasing one of the masses
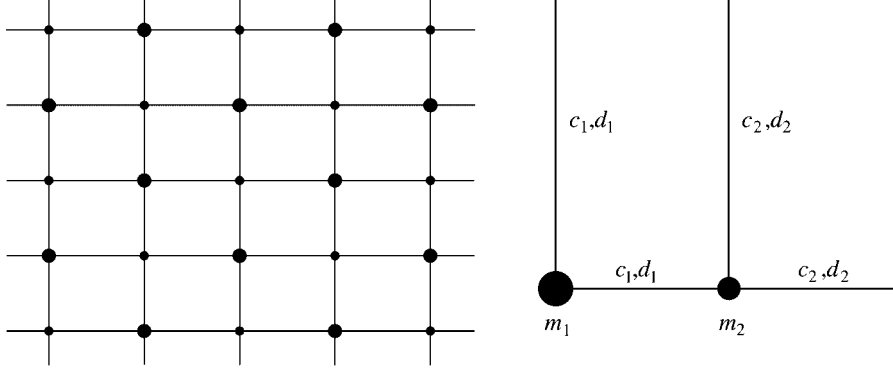
Fig. 10 Square bi-atomic lattice with its irreducible unit cell to the right

while keeping the other one fixed we can push the 'acoustic' modes down in frequency until a band gap appears when $m_2/m_1 \approx 5$. In the right graph of Fig. 8 we illustrate the spectrum for $m_1 = 1$, $m_2 = 10$.

2.2 A bi-atomic square lattice

Next we consider the lattice illustrated in Fig. 10. This structure would be degenerate if bending stiffnesses were disregarded so we need to model it as a frame. To this end we endow the beams with axial stiffnesses c_j and bending stiffnesses d_j, as illustrated in the figure. There are nodes located at points $\mathbf{x}^1 = (0, 0)$ and $\mathbf{x}^2 = (l, 0)$ in the unit cell, these nodes have masses m_κ and polar moments of inertia J_κ, for $\kappa = 1, 2$. We use the same notation as in the previous example but note that now the lattice vectors are given by $\mathbf{t}^{(1)} = (2l, 0)^{\mathrm{T}}$ and $\mathbf{t}^{(2)} = (l, l)^{\mathrm{T}}$. We also need to include a rotational degree of freedom to the nodal displacements, $\mathbf{u}^{(\mathbf{n},\kappa)} = (u_1^{(\mathbf{n},\kappa)}, u_2^{(\mathbf{n},\kappa)}, u_{\mathrm{rot}}^{(\mathbf{n},\kappa)})^{\mathrm{T}}$.

The equations of motion will this time constitute a set of three equations for each node, two for the components of the momentum and one for the angular momentum. The process of writing these down and combining them with the quasi-periodicity condition is straightforward but somewhat lengthy so we leave it to Appendix B. The end result is an equilibrium equation of the form (4), where now $M = \mathrm{diag}\{m_1, m_1, J_1, m_2, m_2, J_2\}$ and the stiffness matrix $\sigma(\mathbf{k})$ consists of four 3×3 blocks whose entries depend on the axial and bending stiffnesses c_j and d_j.

The dispersion equation, which again takes the form (5), has been solved numerically, and in Fig. 11 we show some characteristic dispersion diagrams. Note that the slope of the lowest acoustic line is far lower when going from A to B than it is when going from B to C. This is a manifestation of the strong anisotropy of this material. The plot also indicates the existence of a large band gap, whose existence is verified by the projection of the surfaces $\omega = \omega(k_1, k_2)$ given in Fig. 12.

3. Periodic structures of general geometry

A general lattice geometry in $\mathbb{R}^d$ can be specified by the following objects.
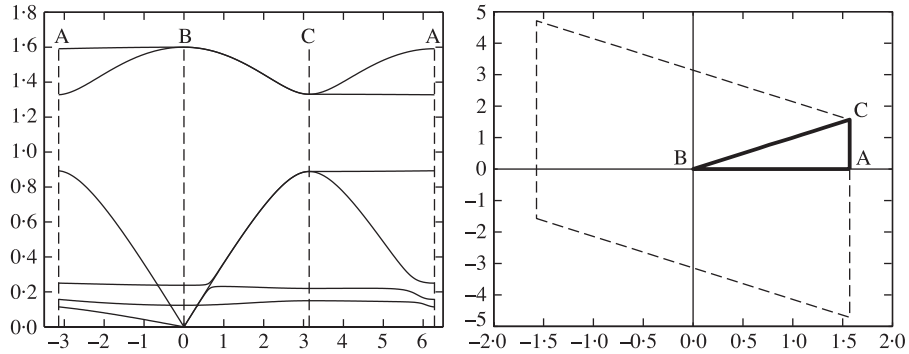
Fig. 11 Dispersion curves for the square, bi-atomic lattice along the contour illustrated to the right. The constants are $c_1 = 1$, $c_2 = 2$, $d_1 = 0.002$, $d_2 = 0.004$, $m_1 = 2$, $m_2 = 3$, $J_1 = 1$, $J_2 = 2$
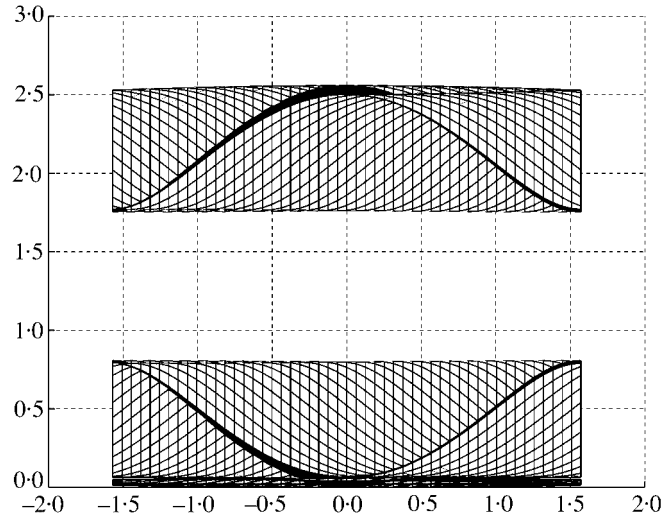
Fig. 12 Surface plots of the functions $\omega(\mathbf{k})$ viewed along the $k_1 = 0$ axis

Reference cell. We specify an irreducible reference cell $\Omega \subset \mathbb{R}^d$ in the form of a parallelepiped spanned by some *translation vectors* $\mathbf{t}^{(i)} \in \mathbb{R}^d$, $1 \leqslant i \leqslant d$. Then its translates

$$\bigcup_{\mathbf{n} \in \mathbb{Z}^d} \left(\Omega + \sum_{i=1}^d n_i \mathbf{t}^{(i)} \right)$$

will form a disjoint covering of $\mathbb{R}^d$. We frequently collect the translation vectors in a matrix $T = [\mathbf{t}^{(1)}, \ldots, \mathbf{t}^{(d)}]$. Then, for $\mathbf{n} \in \mathbb{Z}^d$ label the set $\Omega^{(\mathbf{n})} = \Omega + T\mathbf{n}$ as 'cell $\mathbf{n}$'.

Nodes. Let $\{\mathbf{x}^{\kappa}\}_{\kappa=1}^{q} \subset \omega$ be the *nodes* in the reference cell. We use the notation $\mathbf{x}^{(\mathbf{n},\kappa)} = \mathbf{x}^{\kappa} + T\mathbf{n}$ to index nodes in the lattice by giving their node number κ and the label of the cell they belong to, $\mathbf{n}$.

Lattice members. Finally we specify a list of b lattice members $\{(\kappa_j, \mathbf{n}_j, \lambda_j)\}_{j=1}^{b}$, where for each member we specify the node $\mathbf{x}^{\kappa_j}$ (in the reference cell) that it starts from, and the node $\mathbf{x}^{(\mathbf{n}_j, \lambda_j)}$ it connects to.

For convenience we define two index sets:

$$\mathbb{B}_{\kappa} = \{(\mathbf{n}, \lambda)\} \text{ is a list of nodes } (\mathbf{n}, \lambda) \text{ connected to the node } (0, \kappa), \text{ and}$$

$$\mathbb{B}_{\kappa\lambda} = \{\mathbf{n}\} \text{ is a list of the indices } \mathbf{n} \text{ such that } (0, \kappa) \text{ connects to } (\mathbf{n}, \lambda).$$

It is easy to verify that

$$(\mathbf{n}, \lambda) \in \mathbb{B}_{\kappa} \quad \Leftrightarrow \quad \mathbf{n} \in \mathbb{B}_{\kappa\lambda} \quad \Leftrightarrow \quad -\mathbf{n} \in \mathbb{B}_{\lambda\kappa} \quad \Leftrightarrow \quad (-\mathbf{n}, \kappa) \in \mathbb{B}_{\lambda}.$$

Introduce the variable $\mathbf{u}^{(\mathbf{n},\kappa)}$ to denote the 'displacement' of node $(\mathbf{n}, \kappa)$. The term displacement should be interpreted in a generalized sense since depending on context it may model either the temperature at the node or translational and/or rotational degrees of freedom of a mechanical structure. Assumimg that the 'load-displacement' relationship is linear for each lattice member we write equilibrium for the member of type $(\kappa, \mathbf{m}, \lambda)$ that connects $(\mathbf{n}, \kappa)$ to $(\mathbf{n} + \mathbf{m}, \lambda)$ as

$$\begin{bmatrix} \mathbf{f}^{(1)} \\ \mathbf{f}^{(2)} \end{bmatrix} = A^{(\kappa,\mathbf{m},\lambda)} \begin{bmatrix} \mathbf{u}^{(\mathbf{n},\kappa)} \\ \mathbf{u}^{(\mathbf{n}+\mathbf{m},\lambda)} \end{bmatrix} = \begin{bmatrix} A_{11}^{(\kappa,\mathbf{m},\lambda)} & A_{12}^{(\kappa,\mathbf{m},\lambda)} \\ A_{21}^{(\kappa,\mathbf{m},\lambda)} & A_{22}^{(\kappa,\mathbf{m},\lambda)} \end{bmatrix} \begin{bmatrix} \mathbf{u}^{(\mathbf{n},\kappa)} \\ \mathbf{u}^{(\mathbf{n}+\mathbf{m},\lambda)} \end{bmatrix},$$

where $\mathbf{f}^{(1)}$ and $\mathbf{f}^{(2)}$ are the (generalized) forces acting at the ends of the member. The matrices $A^{(\kappa,\mathbf{m},\lambda)}$ should all be non-negative and symmetric (to conform with Castigliano's theorems). Since the lattice is periodic we must also have

$$A_{12}^{(\kappa,\mathbf{m},\lambda)} = (A_{12}^{(\lambda,-\mathbf{m},\kappa)})^{\mathrm{T}}, \qquad A_{11}^{(\kappa,\mathbf{m},\lambda)} = A_{22}^{(\lambda,-\mathbf{m},\kappa)}. \tag{6}$$

Newton's second law for the node $(\mathbf{n}, \kappa)$ takes the form

$$\mathbf{f}^{(\mathbf{n},\kappa)} = M^{\kappa} \ddot{\mathbf{u}}^{(\mathbf{n},\kappa)} + \sum_{(\mathbf{m},\lambda)\in\mathbb{B}_{\kappa}} \left[A_{11}^{(\kappa,\mathbf{m},\lambda)} \mathbf{u}^{(\mathbf{n},\kappa)} + A_{12}^{(\kappa,\mathbf{m},\lambda)} \mathbf{u}^{(\mathbf{n}+\mathbf{m},\lambda)} \right], \tag{7}$$

where M^{κ} is a mass-matrix corresponding to masses lumped at node $\mathbf{x}^{(\mathbf{n},\kappa)}$. The equation is of convolution form and it is therefore easily diagonalizable by the Fourier transform

$$\mathcal{F} : u \rightarrow \tilde{u}(\mathbf{k}) = \sum_{\mathbf{n}\in\mathbb{Z}^d} e^{i\mathbf{x}^{(\mathbf{n})}\cdot\mathbf{k}} \mathbf{u}^{(\mathbf{n})}, \quad \text{for } \mathbf{k} \in T^{-\mathrm{T}}[-\pi, \pi]^d,$$

where $\mathbf{x}^{(\mathbf{n})} = T\mathbf{n}$. We find that

$$\tilde{\mathbf{f}}^{\kappa}(\mathbf{k}) = M^{\kappa} \partial_t^2 \tilde{\mathbf{u}}(\mathbf{k}) + \sum_{(\mathbf{m},\lambda)\in\mathbb{B}_{\kappa}} \left[A_{11}^{(\kappa,\mathbf{m},\lambda)} \tilde{\mathbf{u}}^{\kappa}(\mathbf{k}) + A_{12}^{(\kappa,\mathbf{m},\lambda)} e^{-i\mathbf{x}^{(\mathbf{m})}\cdot\mathbf{k}} \tilde{\mathbf{u}}^{\lambda}(\mathbf{k}) \right]$$

$$= M^{\kappa} \partial_t^2 \tilde{\mathbf{u}}(\mathbf{k}) + \sum_{\lambda=1}^{q} \sum_{\mathbf{m}\in\mathbb{B}_{\kappa\lambda}} \left[A_{11}^{(\kappa,\mathbf{m},\lambda)} \delta_{\kappa\lambda} + e^{-i\mathbf{x}^{(\mathbf{m})}\cdot\mathbf{k}} A_{12}^{(\kappa,\mathbf{m},\lambda)} \right] \tilde{\mathbf{u}}^{\lambda}(\mathbf{k}).$$

Write $\tilde{\mathbf{u}}(\mathbf{k}) = [\tilde{\mathbf{u}}^1(\mathbf{k}), \ldots, \tilde{\mathbf{u}}^q(\mathbf{k})]^T$ and $\tilde{\mathbf{f}}(\mathbf{k}) = [\tilde{\mathbf{f}}^1(\mathbf{k}), \ldots, \tilde{\mathbf{f}}^q(\mathbf{k})]^T$, and introduce a matrix $\sigma(\mathbf{k})$ whose $\kappa\lambda$-block is given by

$$\sigma_{\kappa\lambda}(\mathbf{k}) = \sum_{\mathbf{m}\in\mathbb{B}_{\kappa\lambda}} \left[A_{11}^{(\kappa,\mathbf{m},\lambda)}\delta_{\kappa\lambda} + e^{-i\mathbf{x}^{(\mathbf{m})}\cdot\mathbf{k}} A_{12}^{(\kappa,\mathbf{m},\lambda)} \right], \tag{8}$$

and let $M = \text{diag}\{M^\kappa\}_{\kappa=1}^q$ be the mass-matrix. Then (7) can be written in diagonal form as

$$\tilde{\mathbf{f}}(\mathbf{k}) = M\partial_t^2\tilde{\mathbf{u}}(\mathbf{k}) + \sigma(\mathbf{k})\tilde{\mathbf{u}}(\mathbf{k}).$$

Looking for harmonic waves we set the forcing to zero, substitute $-\omega^2\tilde{\mathbf{u}}(\mathbf{k})$ for $\partial_t^2\tilde{\mathbf{u}}(\mathbf{k})$, and find the eigenvalue problem

$$\left[\sigma(\mathbf{k}) - \omega^2 M\right]\tilde{\mathbf{u}}(\mathbf{k}) = 0. \tag{9}$$

The following proposition guarantees that the solutions ω^2 are all real and non-negative: *the symbol $\sigma(\mathbf{k})$ is a Hermitian, non-negative matrix.*

To prove this we start with (8) and, using (6), we find that

$$[\sigma_{\kappa\lambda}(\mathbf{k})]^\star = \sum_{\mathbf{m}\in\mathbb{B}_{\kappa\lambda}} \left[[A_{11}^{(\kappa,\mathbf{m},\lambda)}\delta_{\kappa\lambda}]^T + e^{i\mathbf{x}^{(\mathbf{m})}\cdot\mathbf{k}}[A_{12}^{(\kappa,\mathbf{m},\lambda)}]^T \right]$$

$$= \sum_{\mathbf{m}\in\mathbb{B}_{\kappa\lambda}} \left[A_{11}^{(\kappa,\mathbf{m},\lambda)}\delta_{\kappa\lambda} + e^{i\mathbf{x}^{(\mathbf{m})}\cdot\mathbf{k}} A_{12}^{(\lambda,-\mathbf{m},\kappa)} \right] = \sigma_{\lambda\kappa}(\mathbf{k}),$$

where in the last step we used that $\mathbf{m}\in\mathbb{B}_{\kappa\lambda} \Leftrightarrow -\mathbf{m}\in\mathbb{B}_{\lambda\kappa}$. This proves that $\sigma(\mathbf{k})$ is Hermitian. To prove the non-negativeness claim, fix any test function $\tilde{\mathbf{u}}$ and set $\mathbf{u} = \mathcal{F}^{-1}[\tilde{\mathbf{u}}]$. Then by Parseval's theorem

$$\int_{T^{-T}(-\pi,\pi)^d} (\tilde{\mathbf{u}}(\mathbf{k}))^\star\sigma(\mathbf{k})\tilde{\mathbf{u}}(\mathbf{k})\,d\mathbf{k}$$

$$= (2\pi)^d \sum_{\mathbf{n}\in\mathbb{Z}^d} \sum_{j=1}^b \left[\begin{matrix} \mathbf{u}^{(\mathbf{n},\kappa_j)} \\ \mathbf{u}^{(\mathbf{n}+\mathbf{m}_j,\lambda_j)} \end{matrix} \right]^T A^{(\kappa_j,\mathbf{m}_j,\lambda_j)} \left[\begin{matrix} \mathbf{u}^{(\mathbf{n},\kappa_j)} \\ \mathbf{u}^{(\mathbf{n}+\mathbf{m}_j,\lambda_j)} \end{matrix} \right] \geqslant 0$$

since all the local matrices are non-negative.

In the context of mechanical lattices we earlier made the distinction between truss and frame structures. For the truss structures we study only the translational degrees of freedom so that $\mathbf{u}^{(\mathbf{m},\kappa)} \in \mathbb{R}^d$. The stiffness matrix of a bar with cross-section s, length l, Young's modulus E and oriented along the unit vector $\mathbf{a}$ will be given by

$$A = \frac{sE}{l} \left[\begin{matrix} \mathbf{a}\mathbf{a}^T & -\mathbf{a}\mathbf{a}^T \\ -\mathbf{a}\mathbf{a}^T & \mathbf{a}\mathbf{a}^T \end{matrix} \right].$$

The mass of a bar is proportional to $sl\rho$ where ρ is the density of the base material. Looking at the dispersion equation (9) we then determine the typical frequency ω_{truss} of the eigenmodes of the truss, $sE/l \sim \omega_{\text{truss}}^2 sl\rho$, so that

$$\omega_{\text{truss}} \sim l^{-1}\sqrt{E/\rho}. \tag{10}$$

Recalling that elastic waves in the base material travel with a group velocity proportional to $\sqrt{E/\rho}$

we find that this frequency corresponds to waves in the base material with a wavelength equal to the cell size. Note in particular that the cross-sectional area of the bars cancels.

For frame structures the situation is somewhat more complicated, even when we restrict attention to two-dimensional structures. For a beam oriented along the x_1-axis with cross-sectional area s and cross-sectional moment of inertia I the equilibrium equation reads

$$
\begin{bmatrix} f_1^1 \\ f_2^1 \\ T^1 \\ \hline f_1^2 \\ f_2^2 \\ T^2 \end{bmatrix} = \left[\begin{array}{ccc|ccc} sE/l & 0 & 0 & -sE/l & 0 & 0 \\ 0 & 6\gamma & 3\gamma l & 0 & -6\gamma & 3\gamma l \\ 0 & 3\gamma l & 2\gamma l^2 & 0 & -3\gamma l & \gamma l^2 \\ \hline -sE/l & 0 & 0 & sE/l & 0 & 0 \\ 0 & -6\gamma & -3\gamma l & 0 & 6\gamma & -3\gamma l \\ 0 & 3\gamma l & \gamma l^2 & 0 & -3\gamma l & 2\gamma l^2 \end{array} \right] \begin{bmatrix} u_1^1 \\ u_2^1 \\ \theta^1 \\ \hline u_1^2 \\ u_2^2 \\ \theta^2 \end{bmatrix}, \tag{11}
$$

where $\gamma = 2EI/l^3$. Here we labelled the two ends of the beam 1 and 2 and let (f_1^j, f_2^j, T^j) denote the forces and moments acting at end j, and similarly (u_1^j, u_2^j, θ^j) denote the translational and rotational degrees of freedom of the displacement at end j. We commonly work with non-dimensional entities in which case (11) takes the form (writing it only for node 1),

$$
\begin{bmatrix} f_1^1/(sE) \\ f_2^1/(sE) \\ T^1/(slE) \end{bmatrix} = \begin{bmatrix} 1 & 0 & 0 \\ 0 & 6\beta & 3\beta \\ 0 & 3\beta & 2\beta \end{bmatrix} \begin{bmatrix} u_1^1/l \\ u_2^1/l \\ \theta^1 \end{bmatrix} + \begin{bmatrix} 1 & 0 & 0 \\ 0 & -6\beta & 3\beta \\ 0 & -3\beta & \beta \end{bmatrix} \begin{bmatrix} u_1^2/l \\ u_2^2/l \\ \theta^2 \end{bmatrix}, \tag{12}
$$

where $\beta = 2I/(sl^2)$. For a solid bar of width b we have $I \sim b^2 s$ so that $I/(sl^2) \sim (b/l)^2$. For a slender bar the slenderness ratio $\varepsilon = b/l$ is small and the splitting of the stiffness matrix into one part that scales as $O(1)$ and one part that scales as $O(\varepsilon^2)$ is clear. These two parts correspond to axial and bending stiffness, respectively.

Finally we note that the polar moment of inertia of a bar will scale as $m_{\mathrm{bar}}l^2 = \rho s l^3$. We can then estimate the typical frequency of rotational modes from (9), $EI/l \sim \omega_{\mathrm{rot}}^2 J$, so that

$$
\omega_{\mathrm{rot}} \sim \sqrt{\frac{EI}{Jl}} \sim \sqrt{\frac{Esb^2}{\rho s l^4}} \sim \frac{b}{l^2}\sqrt{\frac{E}{\rho}} = \frac{b}{l}\omega_{\mathrm{truss}}
$$

where in the last step we used (10) for ω_{truss}.

4. Designing lattices with prescribed band gaps

In this section we will illustrate how the spectrum of an elastic lattice can be manipulated by introducing certain types of micro-structures. The idea is that the added microstructure should be such that it has its own vibrational modes corresponding to certain types of standing waves in the whole lattice.

As a first example consider a triangular truss structure with an added mass $m_\circ$ at the centre of every other cell, as illustrated in Fig. 13. The mass is suspended by three bars, each with stiffness $c_\circ$. For simplicity we let the basic triangular structure (drawn with thick lines in the figure) have unit masses at the nodes and let it be connected with bars of unit stiffness. In Fig. 14 the effect of the added micro-structure is illustrated. The left graph depicts the spectrum of the original, triangular
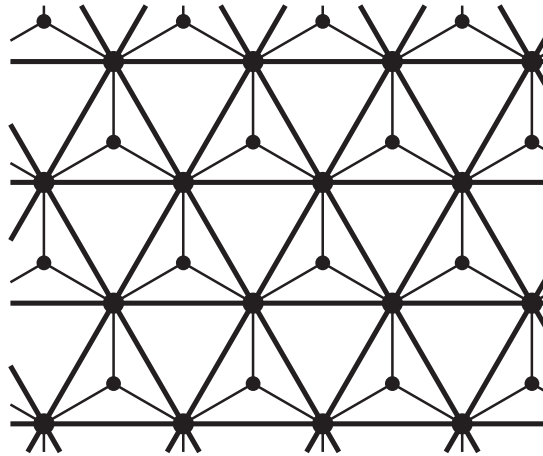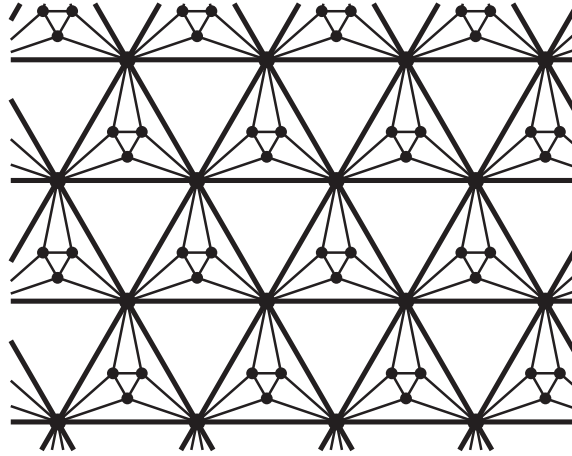
**Fig. 13** Triangular lattice with an oscillator
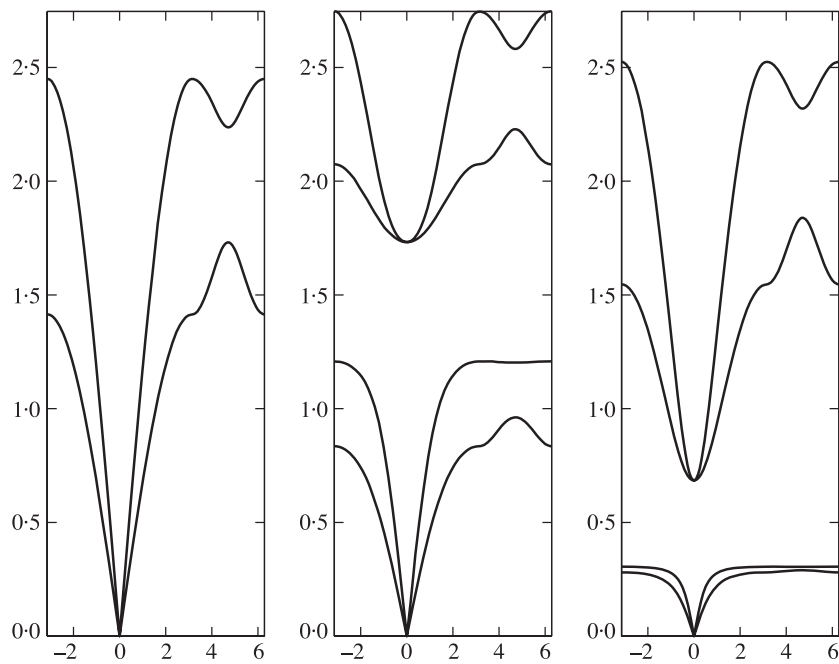
Fig. 14 Spectrum for a triangular truss (left) and the same truss with a simple oscillator (middle and right)

lattice. In the middle graph the micro-structure is included, for $c_\circ = 1$, $m_\circ = 1$. The right graph shows the effect of weakening the springs to $c_\circ = 0.25$ and increasing the internal mass to $m_\circ = 4$. The interesting feature of these graphs is that the added structure clearly has introduced a band gap in the spectrum. Interestingly, we can predict and control the location of this band gap.

Consider a mass $m_\circ$ suspended by three springs with stiffness $c_\circ$, attached to the rigidly fixed

**Fig. 15** Triangular lattice with a complex oscillator
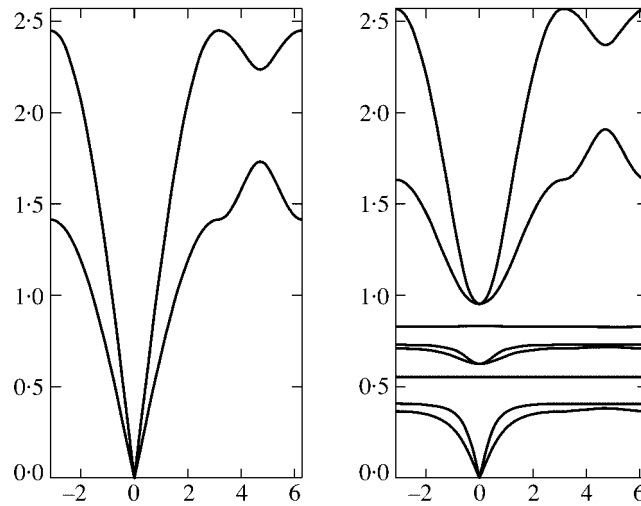
Fig. 16 Spectrum for a triangular truss (left) and the same truss with a complex oscillator (right)

vertices of an equilateral triangle. Using the unit vectors $\mathbf{a}_j$ defined in (3) and letting $\mathbf{u} \in \mathbb{R}^2$ denote the displacement of the mass from the equilibrium point we can write

$$m_\circ \omega^2 \mathbf{u} = c_\circ \left[\mathbf{a}_1 \mathbf{a}_1^{\mathsf{T}} + \mathbf{a}_2 \mathbf{a}_2^{\mathsf{T}} + \mathbf{a}_3 \mathbf{a}_3^{\mathsf{T}} \right] \mathbf{u} = c_\circ \operatorname{diag}\{\tfrac{3}{2}, \tfrac{3}{2}\} \mathbf{u}.$$

This shows that the mass will oscillate about the equilibrium point with a frequency

$$\omega_\circ = \sqrt{3c_\circ/(2m_\circ)}.$$
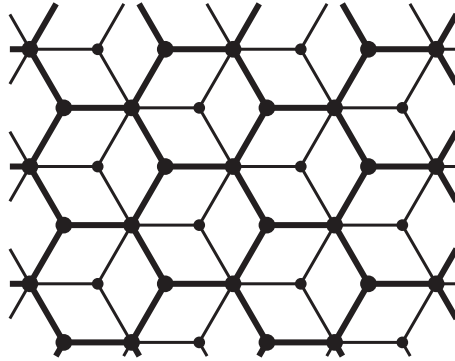
Fig. 17 Honeycomb frame with an oscillator

For the examples illustrated in the graphs, $\{m_\circ, c_\circ\}$ = $\{1, 0.2\}$, $\{5, 0.2\}$ we find $\omega_\circ$ = $\{\sqrt{3/2}, \sqrt{3/32}\} \approx \{1.22, 0.32\}$. These values coincide to a very high degree of accuracy with the lower limits of the band gaps observed in Fig. 14.

Next we consider a more complex oscillator, as illustrated in Fig. 15. In the case illustrated the small internal triangle is 0.15 times the size of the large ones. In Fig. 16 we display the spectrum obtained if all internal nodes have mass 1 and all the internal springs have stiffness 0.2. Doing a calculation similar to the one we did for the simple oscillator in the previous paragraph, we find that the frequencies of the articulated oscillator are $\omega_\circ = \{0.41, 0.41, 0.55, 0.73, 0.73, 0.83\}$. These frequencies match the bands seen in Fig. 16 very well.

Finally we will look at how an oscillator affects the spectrum of a frame structure, as illustrated in Fig. 17. The thick lines representing the original lattice all have unit axial stiffness, a bending stiffness of 0.05 and there are unit masses at the nodes. Then we added another unit mass, $m_\circ = 1$, that is supported by the thin lines, which have an axial stiffness of $c_\circ = 0.2$ but no bending stiffness. This is the same oscillator as in the first example so we expect standing wave modes at $\omega_\circ = \sqrt{3c_\circ/(2m_\circ)} \approx 0.55$, which corresponds exactly to where the new band gap shows up in the right-hand graph in Fig. 18.

5. Conclusions

We have demonstrated that many mechanical lattice structures exhibit complete band gaps, that is, intervals of frequencies for which there are no propagating mechanical waves. We have provided a method for analysis that can be used to quickly determine the band gaps, a method that is easily implemented on a computer for analysis of complicated structures. Finally we have exhibited a method by which lattices can be modified to create complete band gaps at prescribed frequencies.

This work has a wide range of applications in the design of earthquake resistant structures, acoustic mirrors, filters and acoustic lasers.
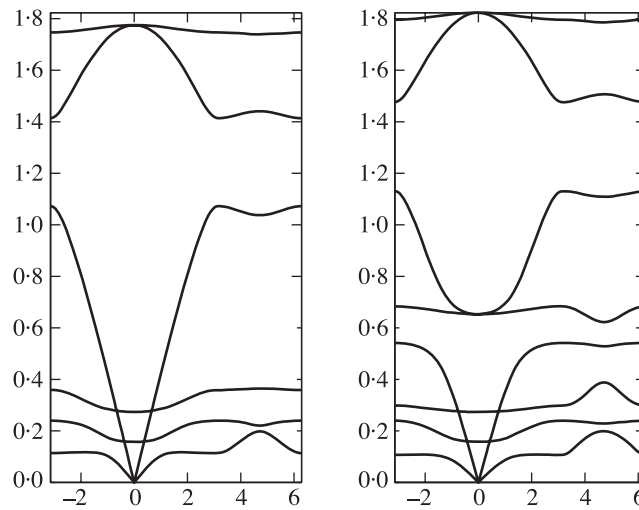
Fig. 18 Spectrum for the honeycomb frame (left) and the same frame with an oscillator (right)

References

1. C. Kittel, *Introduction to Solid State Physics,* 7th edn (Wiley, New York 1996).
2. L. Brillouin, *Wave Propagation in Periodic Structures,* 2nd edn (Dover, New York 1953).
3. J. P. Dowling, H. Everitt and E. Yablonovitch, *Photonic and Sonic Band-Gap Bibliography.* http://home.earthlink.net/jpdowling/pbgbib.html, 2000.
4. M. M. Sigalas and E. N. Economou, Elastic and acoustic wave band structure, *J. Sound Vibr.* **158** (1992) 377–382.
5. ——and ——, Elastic waves in plates with periodically place inclusions, *J. Appl. Phys.* **75** (1994) 2845–2850.
6. ——and ——, Attenuation of multiple-scattered sound, *Europhys. Lett.* **36** (1996) 241–246.
7. C. G. Poulton, A. B. Movchan, R. C. McPhedran, N. A. Nicorovici and Y. A. Antipov, Eigenvalue problems for doubly periodic structures and phononic band gaps, *Proc. R. Soc.* A **457** (2000) 2561–2568.
8. A. B. Movchan, V. V. Zalipaev and N. V. Movchan, Photonic band gaps for fields in continuous and lattice structures. *IUTAM Symposium on Analytical and Computational Fracture Mechanics of Non-Homogenous Materials,* Cardiff, June 2001, to appear.
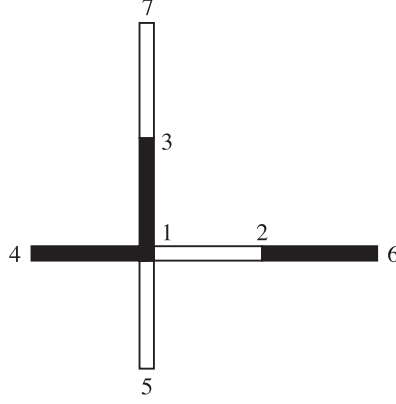
Fig. 19 Labelling used in Appendix A. The white strings have wavespeed v, the black αv. The numbers refer to the nodes

APPENDIX A

Derivation of the dispersion equation (2)

First consider a vibrating string, characterized by its length l and intrinsic velocity v, attached to two supports with the displacements $e^{i\omega t}u^{\mathrm{I}}$ and $e^{i\omega t}u^{\mathrm{II}}$ so that its displacement $w(x)e^{i\omega t}$ is determined by

$$w''(x) + K^2 w(x) = 0, \quad x \in (0, l), \quad w(0) = u^{\mathrm{I}}, \quad w(l) = u^{\mathrm{II}},$$

where $K = \omega/v$. If $\sin Kl \neq 0$, then the solution is

$$w(x) = u^{\mathrm{I}}\cos Kx + (u^{\mathrm{II}} - u^{\mathrm{I}}\cos Kl)(\sin Kx)/(\sin Kl),$$

and thus the dynamic force the string exerts at $x = 0$ is

$$-F\frac{dw}{dx}\bigg|_{x=0} = \frac{FK}{\sin Kl}\left(u^{\mathrm{I}}\cos Kl - u^{\mathrm{II}}\right).$$

Applying the formula above to the system shown in Fig. 19 (which is a part of the big lattice shown in Fig. 5) we get the three equilibrium equations

$$
\begin{aligned}
0 =\ & \frac{FK}{2\sin(Kl/2)}\left(u^{(1)}\cos\frac{Kl}{2} - u^{(2)}\right) + \frac{FK}{2\alpha\sin[Kl/(2\alpha)]}\left(u^{(1)}\cos\frac{Kl}{2\alpha} - u^{(3)}\right) \\
& + \frac{FK}{2\alpha\sin[Kl/(2\alpha)]}\left(u^{(1)}\cos\frac{Kl}{2\alpha} - u^{(4)}\right) + \frac{FK}{2\sin(Kl/2)}\left(u^{(1)}\cos\frac{Kl}{2} - u^{(5)}\right), \\
0 =\ & \frac{FK}{2\sin(Kl/2)}\left(u^{(2)}\cos\frac{Kl}{2} - u^{(1)}\right) + \frac{FK}{2\alpha\sin[Kl/(2\alpha)]}\left(u^{(2)}\cos\frac{Kl}{2\alpha} - u^{(6)}\right), \\
0 =\ & \frac{FK}{2\alpha\sin[Kl/(2\alpha)]}\left(u^{(3)}\cos\frac{Kl}{2\alpha} - u^{(1)}\right) + \frac{FK}{2\sin(Kl/2)}\left(u^{(3)}\cos\frac{Kl}{2} - u^{(7)}\right).
\end{aligned}
\tag{A.1}
$$

We set $c_1 = \cos(Kl/2)$, $s_1 = \sin(Kl/2)$, $c_2 = \cos[Kl/(2\alpha)]$ $s_2 = \sin[Kl/(2\alpha)]$, and apply quasi-periodicity,

$$u^{(4)} = e^{ik_1 l}u^{(2)}, \quad u^{(5)} = e^{ik_2 l}u^{(3)}, \quad u^{(6)} = e^{-ik_1 l}u^{(1)}, \quad u^{(7)} = e^{-ik_2 l}u^{(1)},$$

to reduce the system (A.1) to

$$
\begin{bmatrix} 0 \\ 0 \\ 0 \end{bmatrix} = \begin{bmatrix} 2c_1/s_1 + 2c_2/(\alpha s_2) & -1/s_1 - e^{ik_1 l}/(\alpha s_2) & -1/(\alpha s_2) - e^{ik_2 l}/s_1 \\ -1/s_1 - e^{-ik_1 l}/(\alpha s_2) & c_1/s_1 + c_2/(\alpha s_2) & 0 \\ -1/(\alpha s_2) - e^{-ik_2 l}/s_1 & 0 & c_1/s_1 + c_2/(\alpha s_2) \end{bmatrix} \begin{bmatrix} u^{(1)} \\ u^{(2)} \\ u^{(3)} \end{bmatrix}.
$$

The left-hand side of the dispersion equation (2) is now simply the determinant of the matrix in the system above.

APPENDIX B

Derivation of the stiffness matrix for a square framed structure

In (11) we provided the stiffness matrix for a beam oriented along the x_1-axis, with end-points 1 and 2 to the left and right of the beam, respectively. In the structure illustrated in Fig. 10 there are beams of cross-sectional areas s_1 and s_2, and with moments of intertia I_1 and I_2. We fix a reference area s and define non-dimensional lattice variables $\bar{\mathbf{u}}$ and $\bar{\mathbf{f}}$ by

$$
\bar{u}_j = u_j/l, \quad \bar{f}_j = f_j/(sE), \quad j = 1, 2, \quad \bar{u}_3 = u_{\mathrm{rot}}, \quad \bar{f}_3 = M/(sEl).
$$

Then equilibrium for a beam of type j reads

$$
\begin{bmatrix} \bar{f}_1^1 \\ \bar{f}_2^1 \\ \bar{f}_3^1 \end{bmatrix} = \underbrace{\begin{bmatrix} c_j & 0 & 0 \\ 0 & d_j & \frac{1}{2}d_j \\ 0 & \frac{1}{2}d_j & \frac{1}{3}d_j \end{bmatrix}}_{=:A_j^{0°}} \begin{bmatrix} \bar{u}_1^1 \\ \bar{u}_2^1 \\ \bar{u}_3^1 \end{bmatrix} + \underbrace{\begin{bmatrix} c_j & 0 & 0 \\ 0 & -d_j & \frac{1}{2}d_j \\ 0 & -\frac{1}{2}d_j & \frac{1}{6}d_j \end{bmatrix}}_{=:B_j^{0°}} \begin{bmatrix} \bar{u}_1^2 \\ \bar{u}_2^2 \\ \bar{u}_3^2 \end{bmatrix},
$$

where $c_j = s_j/s$ and $d_j = 12I_j/(sl^2)$. Note that if there had been bars of different lengths in the lattice one would have had to fix a reference length l to use in the non-dimensionalization.

The stiffness matrix for a bar with axial stiffness c_j and bending stiffness d_j, rotated ϕ degrees anti-clockwise from the x_1-axis is given by

$$
A_j^{\phi} = U^{\phi} A_j^{0°} (U^{\phi})^{\mathrm{T}}, \quad B_j^{\phi} = U^{\phi} B_j^{0°} (U^{\phi})^{\mathrm{T}}, \qquad \text{where } U^{\phi} = \begin{bmatrix} \cos\phi & -\sin\phi & 0 \\ \sin\phi & \cos\phi & 0 \\ 0 & 0 & 1 \end{bmatrix}.
$$

We are now in a position to write the equations of motion for the harmonically oscillating square bi-atomic lattice,

$$
\bar{\omega}^2 \bar{M}_1 \bar{\mathbf{u}}^{(\mathbf{n},1)} = \left[A_1^{0°} \bar{\mathbf{u}}^{(\mathbf{n},1)} + B_1^{0°} \bar{\mathbf{u}}^{(\mathbf{n},2)} \right] + \left[A_1^{90°} \bar{\mathbf{u}}^{(\mathbf{n},1)} + B_1^{90°} \bar{\mathbf{u}}^{(\mathbf{n}-\mathbf{e}_1+\mathbf{e}_2,2)} \right]
$$
$$
+ \left[A_2^{180°} \bar{\mathbf{u}}^{(\mathbf{n},1)} + B_2^{180°} \bar{\mathbf{u}}^{(\mathbf{n}-\mathbf{e}_1,2)} \right] + \left[A_2^{270°} \bar{\mathbf{u}}^{(\mathbf{n},1)} + B_2^{270°} \bar{\mathbf{u}}^{(\mathbf{n}-\mathbf{e}_2,2)} \right],
$$
$$
\bar{\omega}^2 \bar{M}_2 \bar{\mathbf{u}}^{(\mathbf{n},2)} = \left[A_2^{0°} \bar{\mathbf{u}}^{(\mathbf{n},2)} + B_2^{0°} \bar{\mathbf{u}}^{(\mathbf{n}+\mathbf{e}_1,1)} \right] + \left[A_2^{90°} \bar{\mathbf{u}}^{(\mathbf{n},2)} + B_2^{90°} \bar{\mathbf{u}}^{(\mathbf{n}+\mathbf{e}_2,1)} \right]
$$
$$
+ \left[A_1^{180°} \bar{\mathbf{u}}^{(\mathbf{n},2)} + B_1^{180°} \bar{\mathbf{u}}^{(\mathbf{n},1)} \right] + \left[A_1^{270°} \bar{\mathbf{u}}^{(\mathbf{n},2)} + B_1^{270°} \bar{\mathbf{u}}^{(\mathbf{n}+\mathbf{e}_1-\mathbf{e}_2,1)} \right],
$$

where $\bar{M}_\kappa = \mathrm{diag}\{m_\kappa/(\rho l s), m_\kappa/(\rho l s), J_\kappa/(\rho s l^3)\}$ and $\bar{\omega} = \omega l/\sqrt{E/\rho}$. Applying quasi-periodicity, $\mathbf{u}^{(\mathbf{n}+\mathbf{m},\kappa)} = e^{i\mathbf{k}\cdot T\mathbf{m}}\mathbf{u}^{(\mathbf{n},\kappa)}$, we obtain

$$
\bar{\omega}^2 \bar{M}_1 \bar{\mathbf{u}}^{(\mathbf{n},1)} = \left[A_1^{0°} + A_1^{90°} + A_2^{180°} + A_2^{270°} \right] \bar{\mathbf{u}}^{(\mathbf{n},1)}
$$
$$
+ \left[B_1^{0°} + e^{-i(lk_1-lk_2)} B_1^{90°} + e^{-2ilk_1} B_2^{270°} + e^{-i(lk_1+lk_2)} B_2^{270°} \right] \bar{\mathbf{u}}^{(\mathbf{n},2)},
$$
$$
\bar{\omega}^2 \bar{M}_2 \bar{\mathbf{u}}^{(\mathbf{n},2)} = \left[A_2^{0°} + A_2^{90°} + A_1^{180°} + A_1^{270°} \right] \bar{\mathbf{u}}^{(\mathbf{n},2)}
$$
$$
+ \left[e^{2ilk_1} B_2^{0°} + e^{-i(lk_1+lk_2)} B_2^{90°} + B_1^{270°} + e^{i(lk_1-lk_2)} B_1^{270°} \right] \bar{\mathbf{u}}^{(\mathbf{n},1)}.
$$

Setting $\bar{M} = \text{diag}\{\bar{M}_1, \ \bar{M}_2\}$ we obtain the equation

$$\sigma(\mathbf{k})\bar{\mathbf{u}}^{(\mathbf{n})} = \bar{\omega}^2 \bar{M}\bar{\mathbf{u}}^{(\mathbf{n})},$$

where the diagonal blocks of the 6×6 Hermitian matrix $\sigma(\mathbf{k})$ are given by

$$\sigma_{11}(\mathbf{k}) = \begin{bmatrix} c_1 + c_2 + d_1 + d_2 & 0 & \frac{1}{2}(d_2 - d_1) \\ 0 & c_1 + c_2 + d_1 + d_2 & \frac{1}{2}(d_1 - d_2) \\ \frac{1}{2}(d_2 - d_1) & \frac{1}{2}(d_1 - d_2) & \frac{2}{3}(d_1 + d_2) \end{bmatrix},$$

$$\sigma_{22}(\mathbf{k}) = \begin{bmatrix} c_1 + c_2 + d_1 + d_2 & 0 & \frac{1}{2}(d_1 - d_2) \\ 0 & c_1 + c_2 + d_1 + d_2 & \frac{1}{2}(d_2 - d_1) \\ \frac{1}{2}(d_1 - d_2) & \frac{1}{2}(d_2 - d_1) & \frac{2}{3}(d_1 + d_2) \end{bmatrix},$$

and the non-zero entries of $\sigma_{12}(\mathbf{k})$ are given by

$$[\sigma_{12}(\mathbf{k})]_{11} = - c_1 - c_2 e^{2ik_1 l} - d_1 e^{i(k_1 l - k_2 l)} - d_2 e^{i(k_1 l + k_2 l)},$$

$$[\sigma_{12}(\mathbf{k})]_{13} = - \tfrac{1}{2} d_1 e^{i(k_1 l - k_2 l)} + \tfrac{1}{2} d_2 e^{i(k_1 l + k_2 l)},$$

$$[\sigma_{12}(\mathbf{k})]_{22} = - c_1 e^{i(k_1 l - k_2 l)} - c_2 e^{i(k_1 l + k_2 l)} - d_1 - d_2 e^{2ik_1 l},$$

$$[\sigma_{12}(\mathbf{k})]_{23} = \tfrac{1}{2} d_1 - \tfrac{1}{2} d_2 e^{2ik_1 l}, \quad [\sigma_{12}(\mathbf{k})]_{31} = \tfrac{1}{2} d_1 e^{i(k_1 l - k_2 l)} - \tfrac{1}{2} d_2 e^{i(k_1 l + k_2 l)},$$

$$[\sigma_{12}(\mathbf{k})]_{32} = - \tfrac{1}{2} d_1 + \tfrac{1}{2} d_2 e^{2ik_1 l},$$

$$[\sigma_{12}(\mathbf{k})]_{33} = \tfrac{1}{6} d_1 (1 + e^{i(k_1 l - k_2 l)}) + \tfrac{1}{6} d_2 (e^{2ik_1 l} + e^{i(k_1 l - k_2 l)}).$$

Note that the bars used to denote non-dimensional variables in this Appendix are not present in the main text since there, all variables are implicitly assumed to be non-dimensional.